SolarPACES 2024, 30th International Conference on Concentrating Solar Power, Thermal, and Chemical Energy Systems

CSP Integration, Markets, and Policy

https://doi.org/10.52825/solarpaces.v3i.2373

Published: 24 Nov. 2025

Hall Effect Focus Control System for Vacuum-Membrane Solar Dish Facets

Duncan S. McGee[1], Willem G. le Roux[1,*], and Evan D. Humphries[1]

[1]University of Pretoria, South Africa

*Correspondence: Willem G. le Roux, willem.leroux@up.ac.za

Abstract. This study investigates the development and implementation of a novel Hall effect focus control system for sensing and maintaining membrane displacement of vacuum-membrane solar dish facets for small-scale concentrating solar power (CSP) systems. Such a CSP system comprises of 46 individual elliptical vacuum-membrane solar-dish facets, each with a variable focal length dependent on the membrane depth. Previous research identified membrane movement as a significant challenge affecting system performance throughout an operating day, due to changing environmental conditions (especially ambient temperature). In response, a cost-effective and low power consumption focus control system utilizing a Hall effect depth sensing method was developed in the current work and mounted to a single facet. Outdoor experimentation on a single facet demonstrated that the control system successfully reduced membrane displacement within an acceptable 0.069 mm/°C accuracy, which is within the required limit of ±2 mm movement for a minimum 90% intercept factor at the solar receiver. Furthermore, by incorporating temperature effects on the Hall effect linear displacement sensor's magnet, a higher accuracy of 0.036 mm/°C was obtained throughout an operating day. These advancements hold promise for enhancing the efficiency and performance of small-scale CSP systems.

Keywords: Hall Effect, Concentrating Solar Power, Focus Control System, Solar Dish, Vacuum-Membrane

1. Introduction

1.1 Background

The University of Pretoria has been actively working on the development of a small-scale concentrating solar power (CSP) systems for the generation of electrical power and process heat [1], [2]. Most recently, the Solar Turbo Combined Heat and Power (ST-CHP) prototype with a dish array comprising of 46 vacuum-membrane solar dish facets and a micro-turbine (see Figure 1) was capable of generating 0.4 kWe during a steady-state on-sun point of interest in the late afternoon and 1.05 kWe during simple-cycle testing [3].Besides heating air as done with ST-CHP [3], the solar dish facets could also be used to melt metals such as zinc. Bezuidenhout and Le Roux [4] determined that six of the current vacuum-membrane solar facets has the potential to process 14.4 kg of zinc per day per m^2 of solar collector surface. Therefore, each facet has the potential to process or recycle 7.74 kg per day. With the current cost of zinc (2.53 USD/kg on the 10th of April 2025), each facet could theoretically provide about 19.5 USD/day. The vacuum-membrane solar dish facets used on ST-CHP were constructed from 0.1-mm-thick EverBright mirror film, from Sundog Solar Technology [5]. The film is adhered to the rim of commercially available elliptical satellite television antennas (80 cm) with a

projected reflective area of 0.538 m^2. By applying a low vacuum within the internal cavity between the membrane and satellite television antenna would deform the membrane into a near-parabolic shape [6]. This deformed membrane shape provides the ability to reflect solar radiation to a specific focal point, depending on the depth of the membrane. Investigations conducted by Swanepoel et al. [7] demonstrated that altering the membrane depth from 25 mm to 5 mm can cause a substantial shift in focal length, ranging from about 2 m to 8 m.

Figure 1. *Vacuum-membrane solar dish array on ST-CHP.*

1.2 Problem

Previous investigations conducted on vacuum-membrane solar dishes indicated that the membrane moved significantly as ambient conditions (especially ambient temperature) changed throughout a normal operating day [8], [9]. Therefore, it was required to reset the membrane depths of 46 facets of the dish-array consistently during the testing of ST-CHP, since the focal length of the reflected solar radiation was greatly affected by the changing membrane depth. This membrane depth movement ultimately caused the dish-array and receiver setup on ST-CHP to have a low intercept factor of 64% [3], which affected the overall efficiency of the small-scaled CSP system.

1.3 Objective

The objective of the current work was to develop a compact, cost-effective, and low-power consumption focus control system to actively sense and maintain the membrane depth within a maximum limit of ±2 mm for a minimum intercept factor of 90%, as determined by Roosendaal et al. [10]. Outdoor experiments were also conducted to test if a single focus control system was able to maintain the membrane depth within the required limit throughout an operating day.

2. Focus control system

2.1 Final design and concept

Similar to other focus control systems, such as the system developed by Butler and Beninga [11], the membrane depth was sensed from the inside of the vacuum-membrane solar dish facet. Butler and Beninga utilized a Linear Variable Differential Transformer (LVDT) to sense the membrane depth for a single large solar dish. However, even though LVDT sensors are very accurate and reliable linear displacement sensors, they are also expensive which would make a focus control system on a 46-facet dish array unfeasible. Therefore, a novel Hall effect linear displacement sensor was developed in the current work with off-the-shelf components

to lower the material and manufacturing costs as much as possible. Hall effect sensors are cost-effective and accurate sensors which can be used as rotation or linear displacement sensors by measuring the movement of a magnet. These sensors convert magnetic strength to a voltage [12], which can be calibrated to displacement as was done by McGee and Le Roux [9].

The novel Hall effect linear displacement sensor was designed to be a replaceable sensor which could be screwed into the back and centre of the satellite television antenna of the vacuum-membrane solar dish facet (see Figure 2). This sensor had a fixed guide with a Hall effect sensor attached to the end of it, allowing the Hall effect sensor to protrude in the vacuum cavity of the facet (see Figure 3). Over the guide was a sleeve with a permanent Neodymium magnet (grade N35) attached to the closed end of the sleeve. This sleeve could easily slide over the fixed guide as the membrane moves up or down. A custom-made low stiffness compression spring always kept the sleeve in contact with the inside of the reflective membrane without affecting the outer smooth surface of the membrane. During standby or defocused conditions (no internal vacuum), the magnet will be at the furthest point away from the Hall effect sensor, as shown in Figure 3 (left). When a low vacuum is applied to deform the membrane, the membrane with a specific pretension will push against the sleeve and compress the spring, allowing the magnet to move closer to the Hall-effect sensor, as shown in Figure 3 (right). This movement of the magnet relative to the Hall effect sensor was used as the input for the control system to determine the exact position of the membrane.

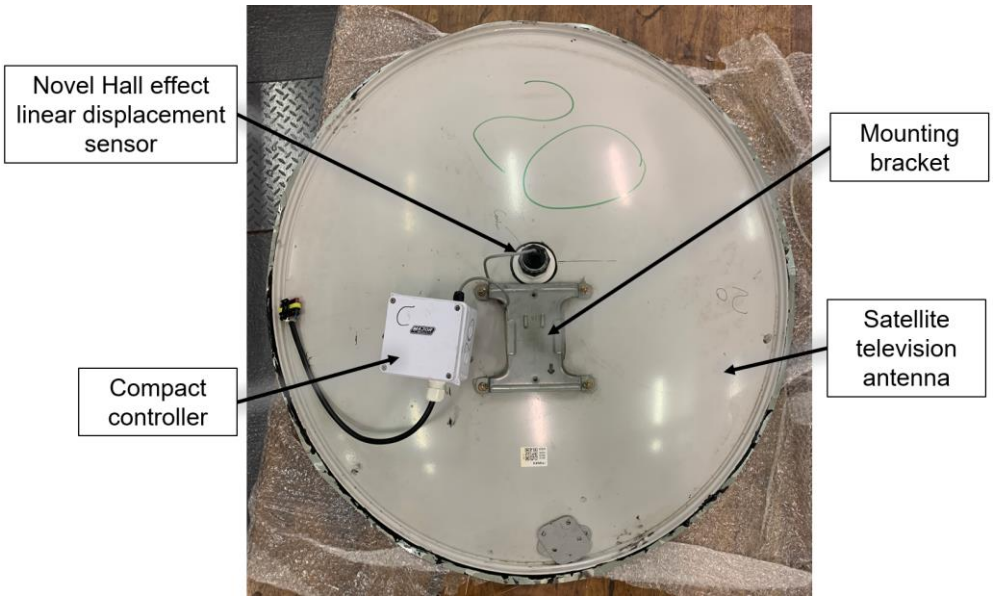

Figure 2. *The novel focus control system mounted the rear of a vacuum-membrane solar dish facet.*

The compact control system comprised a 100 mm x 100 mm x 70 mm weatherproof box that screwed onto a pneumatic fitting at the back of the satellite television antenna of the vacuum-membrane solar dish (Figure 2). Inside the weatherproof box were two 5 V diaphragm air pumps, of which one was used as a vacuum pump. These pumps were connected to the pneumatic fitting inside the box with flexible hosing, allowing the pumps to change the air volume of the internal cavity of a facet. The two pumps were connected to a 2-channel relay module (5 V), which was controlled by an Arduino Nano microcontroller. The novel Hall effect linear displacement sensor was connected to a 5 V Hall effect module inside the weatherproof box, which sent an analogue voltage signal to the microcontroller. The control system worked with a calibrated target Hall effect value (H_{target}) which correlates to a target membrane depth. The microcontroller verified if the current Hall effect reading was near the target. If the current reading was higher than the corrected target, the microcontroller would activate the relay to switch on the air pump. This would then push the membrane up, allowing the sleeve to move up and magnet further away from the Hall effect sensor. If the current reading was lower than the

target membrane depth, the microcontroller would activate the relay to switch on the air vacuum-pump. This would then pull the membrane down, allowing the sleeve to move down and the magnet closer to the Hall-effect sensor.

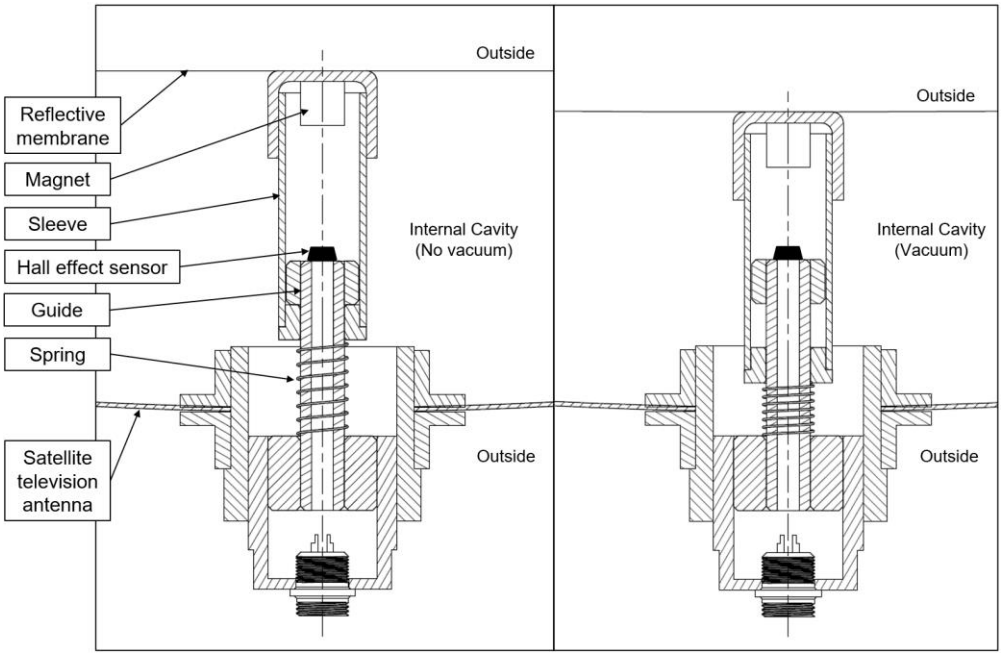

Figure 3. *Hall effect linear displacement schematic (sectioned for clarity), Left – defocused facet, Right – focused facet.*

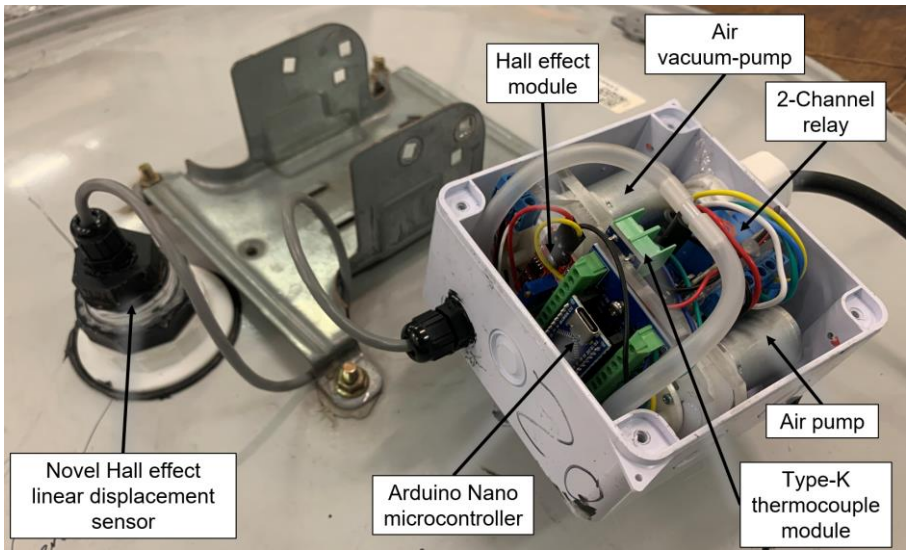

Figure 4. *Compact focus control system inside the weatherproof box (excluding the lid).*

During the initial testing, and as will be indicated in Section 3, there was still some membrane movement with this control system in operation. It was expected that this movement was related to the magnetism of the Neodymium magnet (grade N35) being affected by changing temperatures. According to the manufacturer's datasheet [13], the magnetism decreases by 0.11%/˚C (*c*) for every degree Celsius of temperature increase, and vice versa. This is true up to the Curie temperature of 80˚C, where the magnet will permanently loose magnetism [13]. Therefore, a 5 V type-K thermocouple module was also connected to the microcontroller with a type-K thermocouple guided through the flexible hosing and into the vacuum cavity to measure the internal temperature which was used to apply a correction factor to the target Hall effect

membrane depth value, as detailed in Equation 1. After every second, the microcontroller adjusted this target Hall effect value (H_{target}) by applying the temperature correction factor, depending on how much the current temperature ($T_{current}$) changed from the initial temperature ($T_{initial}$) when the control system was switched on. The microcontroller then verified if the current Hall-effect reading was within the corrected target ($H_{corrected}$) and switched between the air pump and vacuum-pump as required to maintain the corrected target membrane depth. See Figure 4 for more details of the manufactured compact control system inside the weatherproof box.

$$H_{corrected} = H_{target}\,(1 - c\,(T_{current} - T_{initial})) \quad (1)$$

The advantages of the current focus control system are the compactness and cost-effectiveness of the novel Hall effect displacement sensor and control system, which cost USD 80 per prototype facet for materials and labour. This would result in a total cost of 148.6 USD/m^2 for the 46 multifaceted solar dish used on ST-CHP. This is a cost-effective solution for a prototype as a similar sensor used by Butler and Beninga [11] would cost about USD 50 more for just the sensor, excluding the other electronics of the control system. Additionally, the sensor and control system can easily be removed and replaced, reducing potential shutdown time due to maintenance. By actively sensing the membrane depth, the control system also provides the ability to quickly defocus all mirrors in case of an emergency.

2.2 Control system

A simple hysteresis on-off controller (Figure 5) was programmed on the microcontroller as the code could easily be copied and used without adjusting any variables on several vacuum-membrane solar dishes, each with their own sensors, pumps and microcontrollers. A hysteresis band of 0.2% ensured that the system would not overwork itself as the membrane depth was constantly altered past the target depth with the pumps. If the error between the current ($H_{current}$) and corrected ($H_{corrected}$) Hall effect value (see Equation 2) was larger than 0.2%, the vacuum pump would be activated until the next reading. If the subsequent value was less than 0.2%, the air pump would activate until the next reading. If the Hall effect reading was within the ±0.2% hysteresis band, then both pumps would be switched off.

$$e = \frac{H_{current} - H_{corrected}}{H_{corrected}} \quad (2)$$

The total power consumption of one focus control system (Figure 4) was 3.3 W while a pump was switched on. The maximum power consumption when all 46 focus control systems on a dish-array are operating at the same time would be 151.8 W. This low power consumption would be a significant advantage for small-scale CSP systems generating electricity.

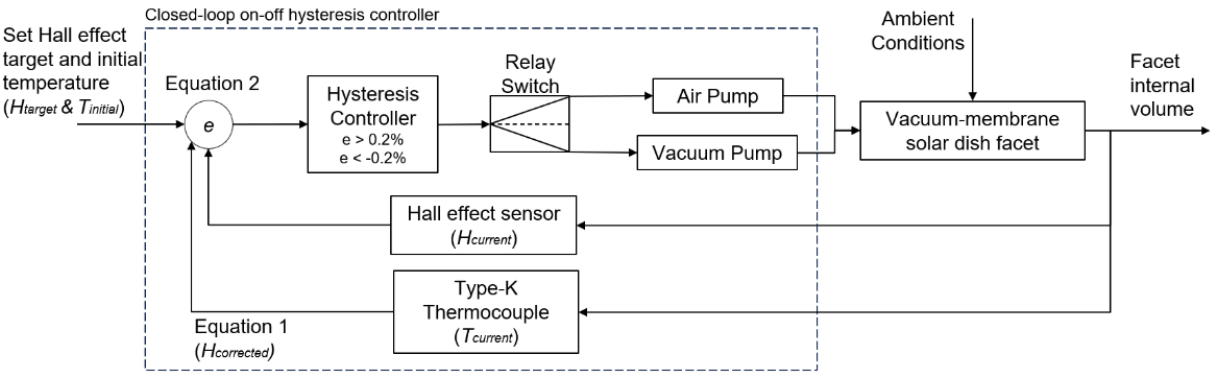

Figure 5. *Block diagram of the hysteresis on-off controller.*

3. Experimental validation

3.1 Methodology

Outdoor experiments had to be conducted to verify if the novel focus control system would be able to sense and maintain the membrane depth within a required maximum displacement of ±2 mm throughout an operating day. The outdoor experiments were conducted as detailed by McGee and Le Roux [9], by placing a single facet outside at an area where there was constant direct sunlight from sunrise to sunset. The external temperature and pressure of the facet was measured with a type-T thermocouple and BMP280 barometric pressure sensor, respectively. The internal temperature and pressure of the facet was measured with a type-T thermocouple and differential pressure transducer, respectively. The membrane depth was also measured from the outside with a calibrated Hall effect sensor and a rod with a magnet at the end moving vertically as the membrane moved (see Figure 6). All variables were recorded every second with a data acquisition system (DAQ) and laptop as soon as the membrane depth was set to 10 mm, and the control system was switched on.

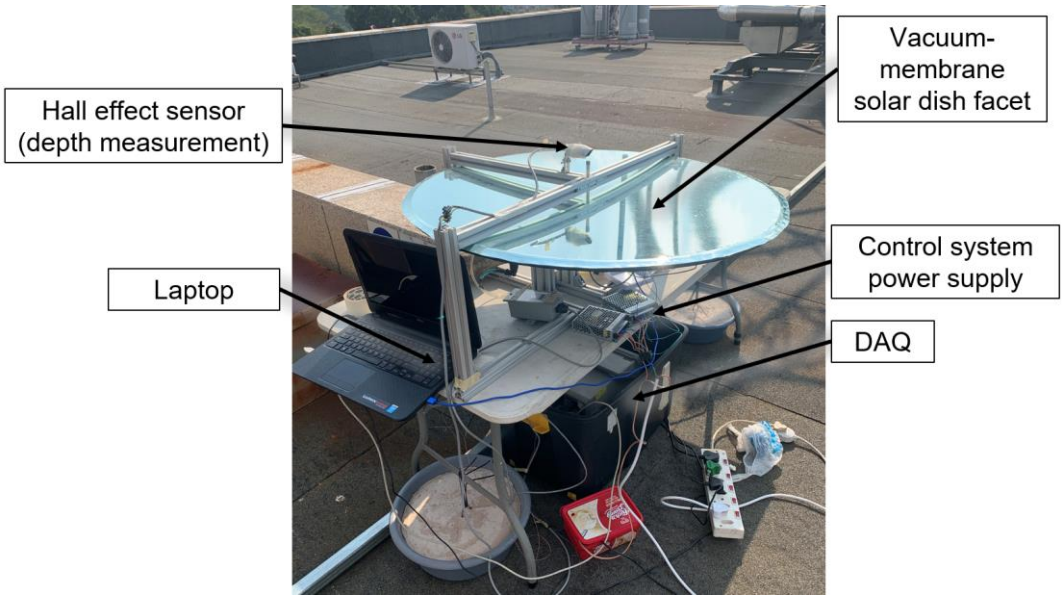

Figure 6. *Outdoor experimental setup.*

3.2 Results

As depicted in Figure 7, the outdoor test without the temperature correction factor started at a membrane depth of 9.8 mm. The depth decreased to about 9.2 mm as the internal facet temperature decreased from 28˚C to 19˚C. The depth then increased to 10.6 mm as the internal temperature increased to 39˚C. It is clear that there was still membrane movement related to changing temperature affecting the magnetism of the Hall effect displacement sensor inside the facet, with a membrane displacement of about 0.069 mm/˚C.

As indicated in Figure 8, the outdoor test with a temperature correction factor of 0.11%/˚C started at a membrane depth of 10.6 mm with an internal facet temperature of 19˚C. The depth increased to a maximum of 11.22 mm as the internal facet temperature increased to 36˚C. This indicated that the temperature correction factor did improve the capability of the control system to maintain the membrane depth, with a membrane displacement of about 0.036 mm/˚C.

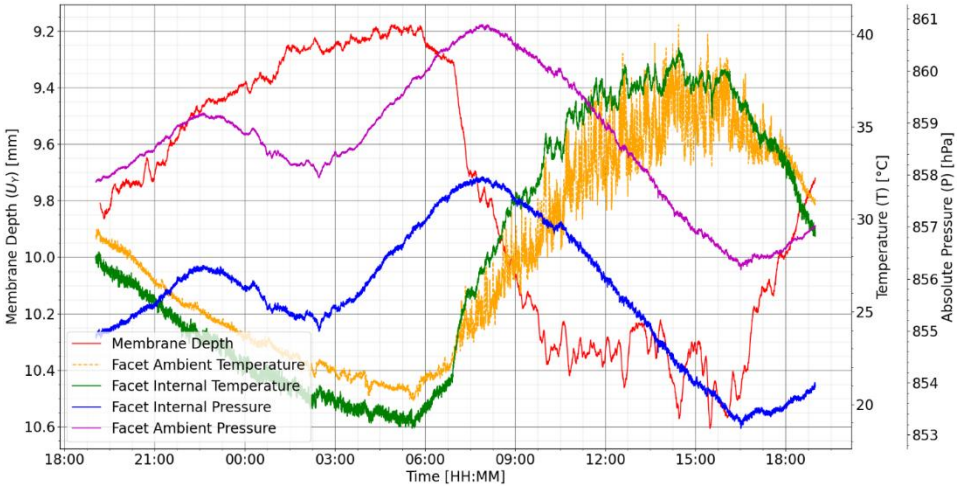

Figure 7. *Outdoor experimental results without the temperature correction factor (5th December 2023).*

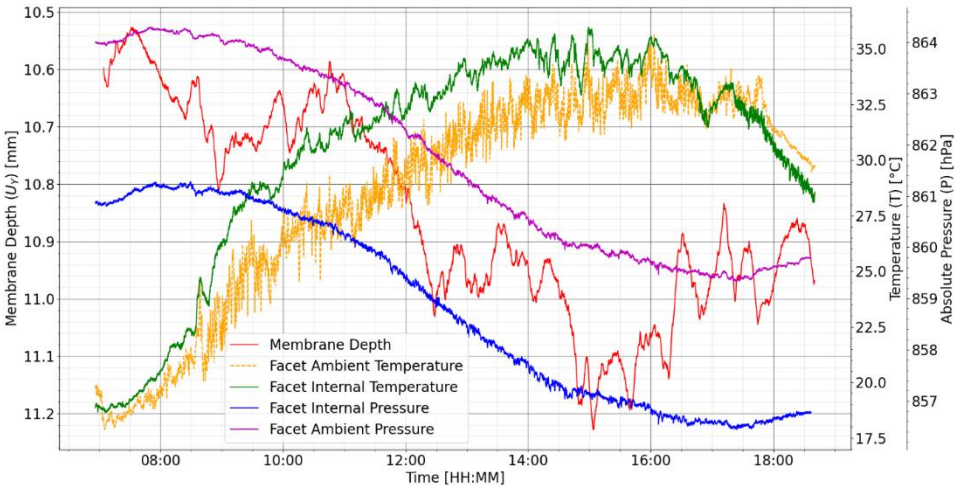

Figure 8. *Outdoor experimental results including the 0.11%/˚C temperature correction factor (16th March 2024).*

4. Conclusion and recommendations

In conclusion, the Hall effect linear displacement sensor with the compact control system at a total cost of USD 80 (148.6 USD/m^2) and power consumption of 3.3 W was able to successfully sense and maintain the membrane depth of a vacuum-membrane solar dish facet within a required ±2 mm limit, which should yield a 90% intercept factor according to Roosendaal et al. [10]. The novel focus control system indicated that the effects of temperature on the magnetism of the Hall effect displacement sensor was important to further lower the membrane displacement to 0.036 mm/˚C, however the control system still performed well within the required limit without the temperature correction factor. Further testing should be conducted on the focus control system on a 46 vacuum-membrane solar dish array, to ultimately develop a method to control individual facets from a main control system. This would allow for the precise depth adjustment on the array as required and to trigger all facets to inflate or defocus in case of an emergency. It is also recommended to conduct further research to improve the durability manufacturing process of the current focus control system design. Different end-cap shapes of the sleeve (see Figure 3) should also be investigated to lower the chance of indenting the reflective membrane surface on facets with lower membrane pretensions.

Data availability statement

The data for the experimental results presented in Section 3 can be accessed at DOI: https://doi.org/10.25403/UPresearchdata.26543512

Author contributions

Duncan S. McGee: Conceptualization, Methodology, Software, Validation, Formal analysis, Investigation, Data Curation, Writing - Original Draft, Visualization, **Willem G. le Roux**: Writing - Review & Editing, Supervision, Funding acquisition, Methodology, **Evan D. Humphries:** Writing - Review & Editing, Methodology

Competing interests

The authors declare the following financial interests/personal relationships which may be considered as potential competing interests: MCGEE DS, LE ROUX WG, Patent Pending, “A position sensor and focus control system”. Reference Number: 2024/06700

Funding

The authors express their gratitude to the Renewable Energy Hub and Spokes Program of the Department of Science and Innovation (DSI) for financial support through the UP Solar Thermal Spoke.

Acknowledgement

The authors would like to acknowledge the contribution of all team members in the UP Solar Thermal Spoke at the University of Pretoria as part of the mobile solar-dish gas-turbine hybrid project.

References

[1] C. Roosendaal, J. K. Swanepoel and W. G. Le Roux, “Performance analysis of a novel solar concentrator using lunar flux mapping techniques,” Solar Energy, vol. 206, pp. 200-215, 2020, DOI: 10.1016/j.solener.2020.05.050.

[2] J. K. Swanepoel, W. G. Le Roux, A. Lexmond and J. Meyer, “Helically coiled solar cavity receiver for micro-scale direct,” Applied Thermal Engineering, vol. 185, p. 116427, 2021, DOI: 10.1016/j.applthermaleng.2020.116427.

[3] J. K. Swanepoel, W. G. Le Roux, C. Roosendaal, S. H. Madani, G. De Wet, T. Nikolaidis, W. Roosendaal, A. Sciacovelli, C. Onorati, Y. Liu, T. S. Mokobodi, D. S. McGee and K. J. Craig, “Initial experimental testing of a hybrid solar-dish Brayton cycle for combined heat and power (ST-CHP),” Applied Thermal Engineering, vol. 249, pp. 123275, 2024, DOI: https://doi.org/10.1016/j.applthermaleng.2024.123275.

[4] P. J. A. Bezuidenhout and W. G. Le Roux, “Solar cavity receiver for melting zinc metal,” Applied Thermal Engineering, vol. 247, pp. 122984, 2024, DOI: https://doi.org/10.1016/j.applthermaleng.2024.122984.

[5] R. C. Gee, “Sundog Solar Technology,” 2023. [Online]. Available: https://www.sundog-solartech.com/. [Accessed 16 September 2023].

[6] L. M. Murphy and C. Y. Tuan, “The formation of optical membrane reflector surfaces using uniform pressure loading,” Solar Energy Research Institute, Report Number SERI/TR-253-3025, Golden, 1987, DOI: https://doi.org/10.2172/6212416.

[7] J. K. Swanepoel, C. Roosendaal and W. G. Le Roux, “Photogrammetry Analysis of a Vacuum-Membrane Solar Dish Using Elliptical Television Antennas,” in Proceedings of the

26th SolarPACES Conference 2020 (online), 28 September - 2 October, 2022, DOI: 10.1063/5.0087025.

[8] D. S. McGee, W. Roosendaal, & W. G. Le Roux, "Environmental Investigation of Vacuum-Membrane Solar-Dish Facets" in Proceedings of the 27th SolarPACES Conference 2021 (online), 27 September - 1 October, 2023, DOI: https://doi.org/10.1063/5.0149745.

[9] D. S. McGee and W. G. Le Roux, "Controlled Static Environment Tests on Vacuum-Membrane Solar-Dish Facets for a Low-Cost Vacuum Control System," in Proceedings of the ISES Solar World Congress (SWC23) 30 October - 4 November 2023, New Delhi, 2024, DOI: https://doi.org/10.18086/swc.2023.03.08.

[10] C. Roosendaal, J. K. Swanepoel and W. G. Le Roux, "Optical modelling of a vacuum-membrane solar dish based on elliptical television antenna", Presented at the Southern African Sustainable Energy Conference (SASEC2021), 17-19 November 2021, Lanzerac Wine Estate, Western Cape, South Africa, 2021. Available: https://sasec.org.za/2021/documents/SASEC_2021_Conference_Proceedings.pdf. [Accessed 22 August 2024].

[11] B. L. Butler and K. J. Beninga, "Focus control system for stretched-membrane mirror module". United States of America Patent 5,016,998, 1991.

[12] J. A. Gaj, "2.04 - Semimagnetic Semiconductors," Comprehensive Semiconductor Science and Technology, vol. 2, pp. 95-124, 2011, DOI: https://doi.org/10.1016/B978-0-44-453153-7.00064-X.

[13] Eclipse Magnetics, "Neodymium Magnets (NdFeB)," 2024. [Online]. Available: https://www.eclipsemagnetics.com/site/assets/files/19485/ndfeb_neodymium_iron_boron-standard_ndfeb_range_datasheet_rev1.pdf. [Accessed 11 August 2024].